THE JOURNAL OF PHYSICAL CHEMISTRY C

ACS AUTHORCHOICE

pubs.acs.org/JPCC Article

Photoinduced Proton-Coupled Electron Transfer in Supramolecular Sn^{IV} Di(L-tyrosinato) Porphyrin Conjugates

Mirco Natali,* Agnese Amati, Sebastiano Merchiori, Barbara Ventura, and Elisabetta Iengo*

Cite This: J. Phys. Chem. C 2020, 124, 8514–8525 Read Online

ACCESS | Metrics & More | Article Recommendations | Supporting Information

ABSTRACT: Proton-coupled electron transfer (PCET) plays a key role in many biological processes, and a thorough comprehension of its subtle mechanistic complexity requires the synthesis and characterization of suitable artificial systems capable of mimicking this fundamental, elementary step. Herein, we report on a detailed photophysical investigation of conjugate **1**, based on a tin(IV) tetraphenylporphyrin (SnTPP) chromophore bound to two L-tyrosinato amino acids, in CH_2Cl_2 in combination with organic bases of different strength and the preparation of a novel conjugate **3**, based on a tin(IV) octaethylporphyrin (SnOEP) in place of the tetraphenyl analogue, and its photophysical characterization in CH_2Cl_2 in the presence of pyrrolidine. In the case of compound **1** with all bases examined, quenching of both the singlet and triplet excited states is observed and attributed to the occurrence of concerted proton−electron transfer (CPET). Rates and quenching yields decrease with the strength of the base used, consistent with the decrease of the driving force for the CPET process. Conjugate **3** with pyrrolidine is quenched only at the triplet level by CPET, albeit with slower rates than its parent compound **1**, ascribable to the smaller driving force as a result of SnOEP being more difficult to reduce than SnTPP. For both systems, the quenching mechanism is confirmed by suitable blank experiments, specific kinetic treatments, and the observation of kinetic isotope effects (KIEs). Differently from what has been previously proposed, a detailed reinvestigation of the triplet quenching of **1** with pyrrolidine shows that no long-lived radical pair state is formed, as diradical recombination is always faster than formation. This is true for both **1** and **3** and for all bases examined. The kinetics of the CPET pathways can be well described according to Marcus theory and point toward the involvement of substantial reorganization energy as typically observed for PCET processes of concerted nature.

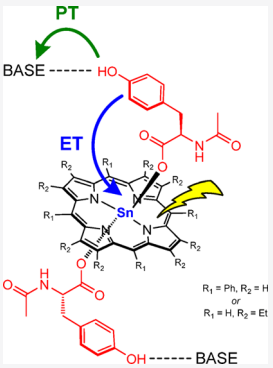

INTRODUCTION

Aromatic amino acids such as tyrosine (TyrOH) play a relevant role as electron transfer (ET) mediators in many biological processes, including, e.g., water oxidation in photosystem II, DNA synthesis, and repair.[1−3] Within this context, oxidation of tyrosine is thought to occur via a proton-coupled electron-transfer (PCET) process. This reactivity is dictated by the intrinsic redox and acid−base properties of the phenol molecule, with the oxidized $TyrOH^{\bullet+}$ cation ($pK_a = -2$ in aqueous solution) capable of easily deprotonating upon electron transfer to give a neutral $TyrO^{\bullet}$ radical.[4] On a mechanistic basis, formation of the tyrosyl radical may occur either via stepwise ET-PT/PT-ET steps or via a concerted mechanism (concerted proton−electron transfer, CPET), with the latter being typically more favorable since it avoids the formation of high energy intermediates.[2,3] When both stepwise and concerted pathways are thermodynamically feasible, competition between these two mechanisms can be observed, and the experimental conditions may play a determining role in selecting one of either ways.

The understanding of the mechanistic complexity at the basis of PCET processes requires the preparation and investigation of suitable artificial analogues. Oxidation of redox-active amino acids has been indeed studied in prototype molecular systems by several research groups, exploiting electrochemical methods,[5,6] chemical oxidants (e.g., polypyridine complexes of transition metals),[7−9] or photogenerated ones (e.g., Ru(III) polypyridines obtained by oxidative quenching of the excited state of Ru(II) complexes in the presence of electron acceptors).[10−13] Albeit less explored than the above-mentioned approaches, the oxidation power of excited states has been also sought as an alternative means to promote PCET.[14−20] This strategy has been recently exploited for the observation, for the first time, of a CPET process in the Marcus inverted region.[21] In such a photoinduced process, the coupled electron−proton motion has to be fast enough to favorably compete with the unimolecular deactivation pathways of the excited state. In this respect, kinetic requirements to achieve an efficient light-induced reaction are relatively more demanding than those of conventional, thermal PCET. Within this framework, we have recently reported on a simple system consisting of a Sn^{IV} porphyrin bearing two tyrosinato

Received: January 9, 2020
Revised: March 11, 2020
Published: April 3, 2020

https://dx.doi.org/10.1021/acs.jpcc.0c00224
J. Phys. Chem. C 2020, 124, 8514−8525

axial ligands (**1**, Chart 1) as a first example of a supramolecular metallo-porphyrin amino acid conjugate.[22] Importantly, differently from the covalent systems typically investigated,[10−18] the supramolecular nature of these type of adducts potentially gives simple, yet direct, access to a considerably extended library of fine-tuned photoactive electron/proton donor/acceptor derivatives, most certainly convenient for gaining new insights into PCET reactivity. For conjugate **1**, excitation of the chromophore with visible light, in CH_2Cl_2 and in the presence of pyrrolidine as a base, was followed by efficient CPET quenching of both the singlet and triplet excited states. In the present work, we have reinvestigated the photophysical properties of conjugate **1** in CH_2Cl_2 in the presence of pyrrolidine in a more detailed manner, combining fast and ultrafast transient absorption techniques. We have also extended the photophysical study of **1** in combination with a series of bases of progressively lower strength (namely, 4-dimethylaminopyridine, pK_a = 17.95 in acetonitrile, 2,4,6-trimethylpyridine, pK_a = 14.98 in acetonitrile, and pyridine, pK_a = 12.53 in acetonitrile).[23] Furthermore, the photophysical properties of a novel supramolecular conjugate, featuring a Sn^{IV}-octaethylporphyrin in place of the Sn^{IV}-tetraphenylporphyrin (**3**, Chart 1), have been investigated in CH_2Cl_2 in the context of photoinduced PCET using pyrrolidine as a base. The main findings can be summarized as follows: (i) differently from what was previously anticipated,[22] CPET quenching of both singlet and triplet excited states does not lead to the formation of long-lived diradical species; (ii) a change in the nature of the base as well as chromophore unit has a remarkable impact on the CPET quenching rates and efficiency; and (iii) the corresponding kinetics can be well correlated assuming a classical Marcus-type treatment for the PCET process.

Chart 1. Molecular Structures of Conjugates 1 and 3 and the Corresponding Model Compounds 2 and 4

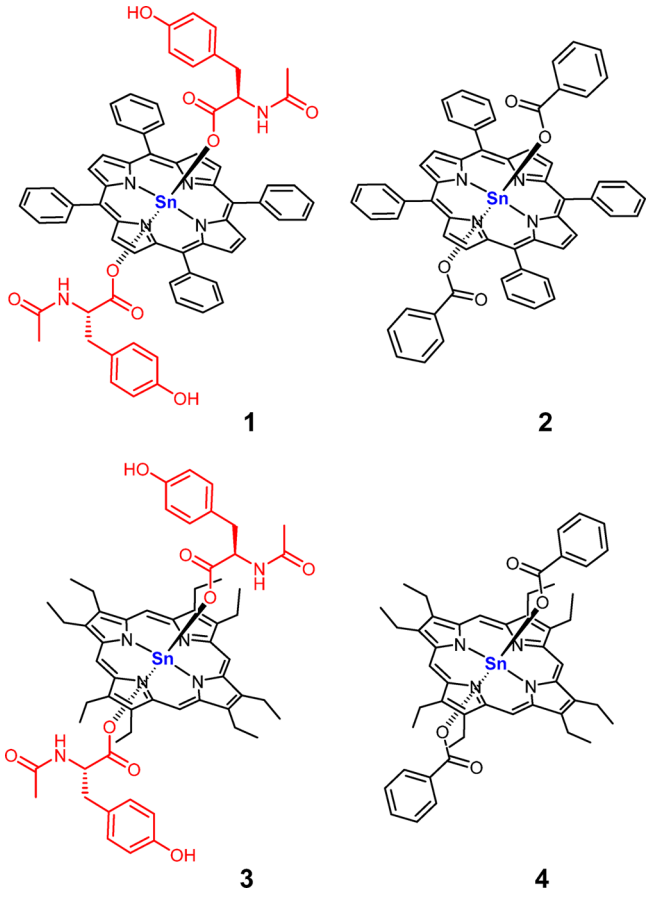

EXPERIMENTAL SECTION

Materials. Chemicals were purchased from Sigma-Aldrich or Alfa Aesar and used without further purification, unless otherwise stated. Solvents for spectroscopic measurements were of spectroscopic grade, and all other chemicals were of reagent-grade quality and used as received.

Apparatus and Procedures. 1D and 2D NMR experiments (^1H, H−H COSY, H−C COSY, H−Sn HMBC) were recorded on a Varian 500 spectrometer (operating at 500 MHz for ^1H, 125 MHz for ^{13}C, and 186 MHz for ^{119}Sn). All spectra were run at room temperature; ^1H and ^{13}C chemical shifts were referenced to the peak of residual nondeuterated solvents: $CDCl_3$ $-\delta$(ppm) = 7.26 and 77.16; DMSO-d_6 $-\delta$(ppm) = 2.5 and 39.52. A ^{119}Sn chemical shift was referenced to the internal standard tetramethyltin at 0.00 ppm. Infrared spectra were recorded on a PerkinElmer FT-IR 2000 spectrometer in the transmission mode, and the samples were prepared as KBr pellets. Electrospray ionization mass spectrometry (ESI-MS) measurements were performed on a Perkin-Elmer APII spectrometer at 5600 eV. Cyclic voltammetry (CV) measurements were carried out with a PC-interfaced Eco Chemie Autolab/Pgstat 30 Potentiostat. Nitrogen-purged 0.5 mM sample solutions in dichloromethane, containing 0.1 M $TBAPF_6$ (tetrabutylammonium hexafluorophosphate, dried in an oven), were used. A conventional three-electrode cell assembly was adopted: a saturated calomel electrode (SCE Amel) and a platinum electrode, both separated from the test solution by a glass frit, were used as the reference and counter (CE) electrodes, respectively; a glassy carbon (GC) electrode was used as the working electrode (WE). UV−vis absorption spectra were recorded on a Cary 300 UV−vis (Agilent Technologies) spectrophotometer. CD spectra were recorded on a JASCO J-815 CD spectrometer, with a 1 mm optical path quartz cuvette. Emission spectra were taken on an Edinburgh Instrument spectrofluorometer equipped with a 900 W Xe arc lamp as an excitation source, a photomultiplier tube, and an InGaAs detector for the visible and the NIR detection, respectively. Fluorescence lifetimes were measured using a TC-SPC apparatus (PicoQuant Picoharp 300) equipped with subnanosecond LED sources (280, 380, 460, and 600 nm and 500−700 ps pulse width) powered by a PicoQuant PDL 800-B variable (2.5−40 MHz) pulsed power supply. The decays were analyzed by means of PicoQuant FluoFit Global Fluorescence Decay Analysis Software. Nanosecond transient measurements were performed with a custom laser spectrometer comprised of a Continuum Surelite II Nd:YAG laser (fwhm 6−8 ns) with frequency doubled (532 nm, 330 mJ) or tripled (355 nm, 160 mJ) options and an Applied Photophysics xenon light source including a model 720 150 W lamp housing, a model 620 power-controlled lamp supply, and a model 03-102 arc lamp pulser. Laser excitation was provided at 90° with respect to the white light probe beam. Light transmitted by the sample was focused onto the entrance slit of a 300 mm focal length Acton SpectraPro 2300i triple grating, flat field, double exit monochromator equipped with a photomultiplier detector (Hamamatsu R3896) and a Princeton Instruments PIMAX II gated intensified CCD camera, using a RB Gen II intensifier, a

https://dx.doi.org/10.1021/acs.jpcc.0c00224
J. Phys. Chem. C 2020, 124, 8514−8525

ST133 controller, and a PTG pulser. Signals from the photomultiplier (kinetic traces) were processed by means of a TeledyneLeCroy 604Zi (400 MHz, 20 GS/s) digital oscilloscope. Transient measurements were performed on oxygen-free solutions obtained by purging with nitrogen gas for ca. 10 min before each experiment.

Ultrafast spectroscopy was performed by means of an Ultrafast Systems HELIOS (HE-VIS-NIR) femtosecond transient absorption spectrometer by using, as an excitation source, a Newport Spectra Physics Solstice-F-1K-230 V laser system, combined with a TOPAS Prime (TPR-TOPAS-F) optical parametric amplifier (pulse width: 100 fs, 1 kHz repetition rate, selected output wavelength: 560 nm). The Solstice system is composed of a tunable (690−1040 nm) Mai Tai HP Ti:Sa femtosecond oscillator, pumped by a Nd:YVO_4 laser (Millennia); a Ti:Sa regenerative amplifier, pumped by an intracavity-doubled, Q-switched, diode-pumped Nd:YLF pulsed laser (Empower 30); an optical pulse stretcher; and an optical pulse compressor. The overall time resolution of the system is 300 fs. Air-equilibrated solutions in 0.2 cm optical path cells (A_{560} = 0.3) were analyzed under continuous stirring. To reduce photodegradation, the pump energy on the sample was reduced to 2 μJ/pulse. Surface Xplorer V4 software from Ultrafast Systems was used for data acquisition and analysis. The 3D data surfaces were corrected for the chirp of the probe pulse prior to analysis.

Synthesis and Characterization. *trans*-Di(*N*-acetyl-L-tyrosinato)(5,10,15,20-tetraphenyl porphyrinato)-tin(IV) (**1**), *trans*-dibenzoato(5,10,15,20-tetraphenylporphyrinato)-tin(IV) (**2**), and *trans*-dibenzoato(2,3,6,7,12,13,16,17-octaethylporphyrinato)-tin(IV) (**4**) were prepared as reported earlier.[22,24] *trans*-Di(*N*-acetyl-L-tyrosinato)(2,3,6,7,12,13,16,17-octaethylporphyrinato)-tin(IV) (**3**) was prepared adapting the previous procedure used for the synthesis of conjugate **1**.[22] *trans*-Dihydroxo(2,3,6,7,12,13,16,17-octaethylporphyrinato)-tin(IV), $SnOEP(OH)_2$ (40 mg, 0.058 mmol), and *N*-acetyl-L-tyrosine (27.4 mg, 0.122 mmol) were dissolved in 40 mL of $CHCl_3$. After stirring at reflux for 12 h, the product formed almost quantitatively as a purple microcrystalline precipitate (57.4 mg, 0.052 mmol, 90% yield). All the relevant characterizations are reported in the Supporting Information (Figures S1−S7). ^{1}H NMR (500 MHz, $CDCl_3$, 5% pyridine-d_5) δ (ppm): 10.53 (s, 4H, Ha), 10.26 (s, 2H, Hj), 6.11 (d, J = 7.8 Hz, 4H, Hi), 4.38 (d, J = 7.8 Hz, 4H, Hh), 4.15 (q, J = 7.7 Hz, 16H, Hb), 3.62 (d, J = 7.4 Hz, 2H, He), 1.89 (t, J = 7.7 Hz, 24H, Hc), 1.03 (q, J = 5.7 Hz, 2H, Hd), 0.84 (s, 6H, Hf), 0.58 (dd, J = 13.2, 5.7 Hz, 2H, Hg), −0.71 (dd, J = 13.1, 3.8 Hz, 2H, Hg). ^{13}C NMR (125 MHz, $CDCl_3$, 5% pyridine-d_5, from HSQC) δ (ppm): 128.60 (Ch), 113.90 (Ci), 97.05 (Ca), 50.62 (Cd), 33.32 (Cg), 21.91 (Cf), 19.68 (Cb), 18.05 (Cc). ^{119}Sn (186 MHz, $CDCl_3$, 5% pyridine-d_5, from HMBC) δ (ppm): −633.3. ^{1}H NMR (500 MHz, DMSO-d_6) δ (ppm): 10.76 (s, 4H, Ha), 8.87 (s, 2H, Hj), 6.15 (d, J = 7.9 Hz, 4H, Hi), 5.80 (d, J = 8.6 Hz, 2H, He), 5.24 (d, J = 7.9 Hz, 4H, Hh), 4.51−3.96 (bs, 16H, Hb), 1.92 (t, J = 7.6 Hz, 24H, Hc), 0.78 (s, 6H, Hf), 0.60−0.47 (bs, 2H, Hd), −0.51 (dd, J = 13.5, Hz, 2H, Hg), −1.39 (d, J = 13.4 Hz, 2H, Hg′). ^{13}C NMR (125 MHz, DMSO-d_6, from HSQC) δ (ppm): 128.1 (Ch), 113.57 (Ci), 97.41 (Ca), 51.71 (Cd), 32.89 (Cg), 20.98 (Cf), 18.69 (Cb), 18.06 (Cc). Selected IR bands (cm^{-1}, KBr pellets): 3432 ($\tilde{\nu}_{OH}$), 1641 ($\tilde{\nu}_{C=O}$). UV−Vis (λ_{max}, nm, CH_2Cl_2): 404 (425 000 M^{-1} cm^{-1}), 499 (2500 M^{-1} cm^{-1}), 536 (19 000 M^{-1} cm^{-1}), 574 (18 500 M^{-1} cm^{-1}). ESI-MS (m/z) (negative mode) for $C_{58}H_{67}N_6O_8Sn_1$ [**3** − 1H$^+$]$^-$ 1095.4, found 1095.5.

RESULTS

Photophysical and Electrochemical Properties in CH_2Cl_2. The absorption spectrum of **1** in CH_2Cl_2 (Figure S8) displays Q-bands with maxima at 518, 557, and 597 nm and a Soret band with a maximum at 423 nm. On the other hand, the absorption spectrum of **3** in CH_2Cl_2 (Figure S9) shows Q-bands with maxima at 499, 536, and 574 nm and the Soret band at 404 nm. In both cases, the additional absorption band with maxima at 276 and 282 nm is attributed to the L-tyrosine amino acids axially bound to the metal center of the porphyrin component. No additional electronic transitions, compared to those of the model compounds **2**, **4**, and *N*-acetyl-tyrosine, can be observed in the UV−vis spectra, suggesting negligible electronic interactions between the porphyrin and the amino acid components. The electrochemical data of **1** and **3**, obtained by cyclic voltammetry (CV), are reported in Table 1 and compared to those of the corresponding models. The close match between the values obtained for each conjugate, the respective model, and the free amino acid additionally confirms the absence of relevant electronic interactions between the two components. This is indeed typical of supramolecular adducts of this kind[24−29] and allows for a facile description of the energetics of the conjugates based on the relevant energy levels of the separate molecular units.

Table 1. Electrochemical Data of Conjugates 1 and 3 and Model Compounds 2 and 4[a]

compound	E_{red} (V)	E_{ox} (V)
1[b]	−1.40	+0.89
2[b]	−1.37	+0.91
3	−1.63	+0.90
4	−1.68	+0.79
N-acetyl-L-tyrosine[b]	/	+0.83

[a]Obtained by cyclic voltammetry (CV) in N_2-purged CH_2Cl_2 with 0.1 M $TBAPF_6$ as supporting electrolyte and scan rate of 0.1 V/s. Potentials are referenced to the Fc/Fc$^+$ couple (see Figures S14 and S15). [b]Taken from ref 22.

Both compounds **1** and **3** in CH_2Cl_2 display intense fluorescence with maxima at 604, 658 nm and 577, 630 nm for **1** and **3**, respectively (Figures S10 and S11). The lifetimes of the singlet excited states (1.14 and 0.90 ns for **1** and **3**, respectively, as measured by TC-SPC) and triplet excited states (ca. 60 and 40 μs for **1** and **3**, respectively, as measured by laser flash photolysis under N_2-purged conditions, Figures S12 and S13, respectively) are comparable to those of the respective model compounds **2** and **4**.[24] This is well explained by examining the redox potentials obtained by CV. For both conjugates, the formation of charge-transfer states involving oxidation of the tyrosine ligand and reduction of the porphyrin component from the excited states of the latter is indeed thermodynamically forbidden (ΔG = +0.10 and +0.45 eV in **1** from the singlet and triplet excited states, respectively, considering an $E^{00}(S_1)$ = 2.10 eV and an $E^{00}(T_1)$ = 1.65 eV;[24,28] ΔG = +0.31 and +0.75 eV in **3** from the singlet and triplet excited states, respectively, considering an $E^{00}(S_1)$ = 2.20 eV and an $E^{00}(T_1)$ = 1.76 eV).[24]

https://dx.doi.org/10.1021/acs.jpcc.0c00224
J. Phys. Chem. C 2020, 124, 8514−8525

Conjugate 1 in CH_2Cl_2 with Pyrrolidine. In our first report on photoinduced PCET with compound **1** in CH_2Cl_2,[22] we employed pyrrolidine as a base (pK_a = 19.56 in acetonitrile)[23] and observed the quenching of both singlet and triplet excited states upon excitation of the porphyrin component in the presence of increasing amounts of pyrrolidine. These quenching processes were assigned to the occurrence of a CPET from both excited states with the formation of $^{1,3}|SnTPP^{\bullet-}-TyrO^{\bullet}|\cdots{}^{+}HPyr$ diradical species. Suitable blank experiments were performed to support the mechanistic assignment.[22] First of all, direct photoreaction with pyrrolidine was excluded since quenching of the singlet excited state by the base in model compound **2** is negligible, while quenching of the triplet is considerably less efficient than in **1**. Second, the occurrence of an ET-only pathway involving a deprotonated phenolate moiety was ruled out since pyrrolidine does not deprotonate the phenol moiety of the *N*-acetyl-L-tyrosine model compound. Also, treatment of the excited-state decay rates according to eq 1, in which k_0 is the rate of the decay in the absence of base, k_Q the bimolecular rate constant for direct excited-state quenching by the base, and K_A the equilibrium constant for the association between the tyrosine and the base (B) via hydrogen bonding,[30] proved to be effective in describing the excited-state decay rates.

$$k_{obs} = k_0 + k_Q[B] + k_{CPET}\frac{K_A[B]}{1 + K_A[B]} \quad (1)$$

In order to calculate the CPET rates for both singlet and triplet quenching pathways, we attempted at fitting the kinetic data of the singlet decay, studied by TC-SPC, and triplet decay, studied by transient absorption spectroscopy, forcing a common value for the association constant in both cases. We now decided to extract more reliable values for both CPET rate constants by calculating the equilibrium constant K_A in a more precise and accurate manner by performing a spectrophotometric titration of model *N*-acetyl-L-tyrosine in CH_2Cl_2 with pyrrolidine paying particular attention to the removal of all the spectral contributions from the added base.[22,31] Furthermore, we decided to employ two different methods for determining the K_A value, the first one used by Mataga and co-workers[32] and the second one by Hammarström and co-workers,[33,34] and to apply both methods to three sets of absorbance values at three different wavelengths around the absorption maximum (see Figures S16–S18). This analysis provided an average value for the association constant of K_A = 33.5 (±1.8) M^{-1} for the hydrogen bonding equilibrium between tyrosine and pyrrolidine. With this value for K_A in hand, the singlet and triplet decay rates of **1** in CH_2Cl_2 have been then fitted as a function of pyrrolidine concentration according to eq 1 (Figures S20 and S21). The bimolecular contribution $k_Q[B]$ has been neglected in the case of the singlet excited-state quenching,[22] whereas for the triplet decay a bimolecular rate constant of k_Q = 9.2(±0.3) × 10^5 M^{-1} s^{-1} (from Stern–Volmer analysis, Figure S19) has been considered. This correlation afforded rate constants of $k_{CPET,S1}$ = 1.9(±0.1) × 10^9 s^{-1} and $k_{CPET,T1}$ = 4.2(±0.2) × 10^6 s^{-1} for the singlet and triplet quenching channels, respectively (Figures S20 and S21), in perfect agreement with those previously determined.[22]

As outlined in our previous report, isolation of a deuterated tyrosinato–porphyrin conjugate, e.g., by treatment of **1** with deuterated methanol,[30] was hampered by the intrinsic instability of the Sn–carboxylate bond in the presence of a large amount of competing oxygen-based ligands. Thus, determination of the kinetic isotope effect (KIE) in pure CH_2Cl_2 resulted to be unfeasible at that stage. We have now looked at the quenching processes of conjugate **1** at both the singlet and triplet level in CH_2Cl_2 with pyrrolidine in the presence of a small amount of either methanol or deuterated methanol (1% v/v).[35] Under these conditions, the exchangeable proton of the tyrosine hydroxide group is expected to be substituted almost quantitatively by the deuteron due to the excess of deuterated methanol. At the same time, the amount of alcohol added (CH_3OH or CD_3OD) is sufficiently modest so that negligible decomposition of the conjugates occurs. Under these conditions, the quenching processes in CH_2Cl_2 with 1% CH_3OH or CD_3OD involving conjugate **1** with pyrrolidine display KIEs of 1.9(±0.2) and 1.4(±0.1) (Figure S22) for the singlet and triplet pathways, respectively. This observation is consistent with the participation of the H/D nuclei in the quenching processes examined, thus confirming the CPET mechanism.[35]

For the products of both CPET quenching pathways, the radical pair state of singlet spin multiplicity was deemed to rapidly recombine within the time scale of the laser flash photolysis apparatus (ca. 10 ns).[22] Thus, in order to look at this process in a more detailed manner, we have now performed ultrafast spectroscopy (UFS) studies. In Figures 1 and 2, respectively, we depict the results obtained on array **1** in CH_2Cl_2 in the absence and in the presence of 0.06 M pyrrolidine upon excitation at 560 nm.

In the absence of pyrrolidine, the spectral changes (Figure 1A) clearly resemble those observed in model compound **2** and are related to the intersystem crossing from the singlet excited state to the triplet.[24,28] The prompt differential spectrum, characteristic of the singlet ^{1}*SnTPP,[24,28] features an absorption with a maximum at 460 nm and a tail at longer wavelengths with superimposed bleaching of the porphyrin Q-bands at 560 and 600 nm and stimulated emission at 600 and 660 nm. This spectrum evolves to a new transient (nice isosbestic points can be seen at 470, 650, and 670 nm, Figure 1A) which displays an absorption with a maximum at 485 nm and a less intense tail at longer wavelengths, these features being characteristic of the triplet ^{3}*SnTPP (Figure S12). The kinetic analysis (Figure 1B) yields a time constant of ca. 1.1 ns, fully consistent with the lifetime of the SnTPP component in model compound **2**.[24,28]

In the presence of pyrrolidine, the prompt spectrum (time delay of 0.1 ps, Figure 2A) still corresponds to the singlet excited state of the SnTPP component. The subsequent spectral evolution is different from that of compound **1** alone yet still monotonic. It shows a general decrease of the absorption features and the loss of the stimulated emission characteristic of the singlet excited state and the subsequent formation of a new transient signal with maximum at 485 nm. The latter spectrum can be clearly assigned to the triplet ^{3}*SnTPP. However, this transient signal is formed in a considerably lower amount than in the case of **1** alone (Figure 1A); furthermore, no isosbestic points are observed for such a conversion. This strongly suggests that most of the singlet excited state has decayed through a new channel in competition with intersystem crossing, namely, via CPET. Kinetic analysis of the singlet excited state decay (Figure 2B) yields a time constant of ca. 390 ps, in fairly good agreement with the lifetime of the SnTPP singlet in **1** measured by TC-

https://dx.doi.org/10.1021/acs.jpcc.0c00224
J. Phys. Chem. C 2020, 124, 8514–8525

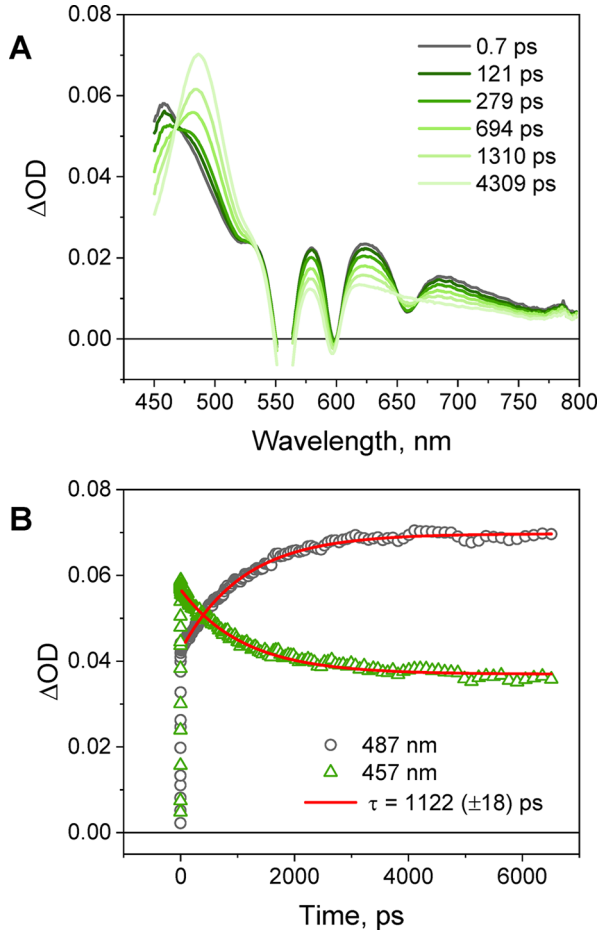

Figure 1. Ultrafast spectroscopy (excitation at 560 nm, 2 μJ) of 70 μM **1** in CH_2Cl_2: (A) spectral evolution and (B) kinetic analyses at 457 and 487 nm.

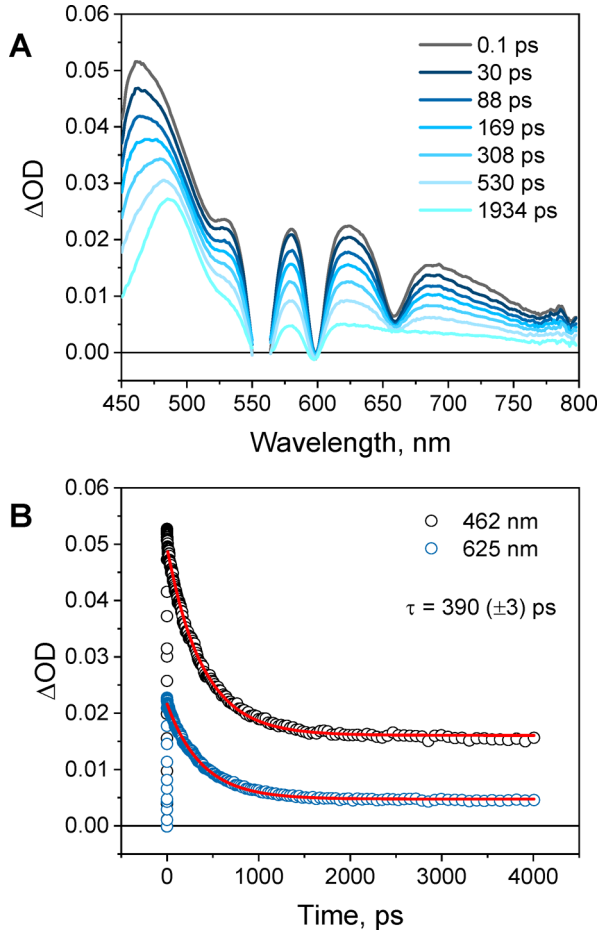

Figure 2. Ultrafast spectroscopy (excitation at 560 nm, 2 μJ) of 70 μM **1** in CH_2Cl_2 in the presence of 0.06 M pyrrolidine: (A) spectral evolution and (B) kinetic analyses at 462 and 625 nm.

SPC under identical conditions (τ = 0.47 ns). The failure to observe any signature from a ^{1}|SnTPP$^{\bullet-}$–TyrO$^{\bullet}$|···$^+$HPyr radical pair state very likely reflects the kinetics of the singlet diradical formation vs recombination, with the former being slower than the latter, so that negligible accumulation of CPET photoproducts can be attained.

As to the product of the triplet CPET quenching, we previously reported[22] that, following the decay of the triplet excited state of the SnTPP component, formation of a long-lived radical pair state of the type ^{3}|SnTPP$^{\bullet-}$–TyrO$^{\bullet}$|···$^+$HPyr occurred. This was indeed consistent with the observation, by laser flash photolysis, of a new transient signal featuring absorption at ca. 450 nm, ascribable to the porphyrin radical anion,[22,36,37] originating from the triplet decay. This transient signal then decayed in ca. 6 μs in deoxygenated solution, and we assigned this process to diradical recombination.[22] The difference of ca. 4 orders of magnitude between the lifetime of the singlet and triplet radical pair states was then explained on the basis of the spin-forbidden nature of the triplet diradical recombination with respect to the singlet pathway. A difference of more than 5 orders of magnitude between the lifetime of singlet and triplet charge-transfer states was indeed observed by Brouwer and co-workers in a compact dyad system based on organic chromophores[38] and attributed to the intrinsic slowness of the singlet–triplet interconversion within the charge-transfer state before charge recombination.[39]

In spite of this potentially sound conclusion, we have pursued a more careful investigation of the triplet decay for both conjugate **1** and model compound **2**. Under the flash photolysis conditions used in the preceding report[22] (i.e., those typically used by us in other studies on porphyrin-based systems,[25−29,40] excitation at 532 nm, and laser power ~20 mJ/pulse), the long-lived transient with maximum at 450 nm observed upon excitation of conjugate **1** in CH_2Cl_2 in the presence of pyrrolidine can be detected even in the absence of the base. Its weight in the overall spectral decay (ca. 4%) is however considerably less pronounced than in **1** with pyrrolidine due to the larger triplet contribution (Figure S23). In both cases, this transient decays with a complex kinetics requiring three exponential functions for a reasonable fit (Figure S24) in which the first (major) component matches the ca. 6 μs lifetime previously measured and assigned to the triplet diradical recombination.[22] This long-lived component is not observed upon excitation of model compound **2** under identical experimental conditions (Figure S25). Altogether these results suggest that this behavior is characteristic of conjugate **1** but at the same time that the long-lived transient detected is *NOT* assignable to the porphyrin radical anion and thus to the formation, via CPET, of a diradical species of triplet spin character, as previously proposed.[22,41] Importantly, the contribution from the transient signal at 450 nm in the spectral evolution of **1** can be minimized upon decreasing the laser power down to 2 mJ/pulse (Figure S27). Under these

https://dx.doi.org/10.1021/acs.jpcc.0c00224
J. Phys. Chem. C 2020, 124, 8514−8525

conditions, the spectral evolution measured by laser flash photolysis of **1** in the presence of 0.065 M pyrrolidine (Figure S21A) is indeed monotonic, showing a fast decay of the SnTPP triplet to the baseline. No trace of a long-lived component can be discerned, and the decay can be attributed to the forward CPET process from the triplet excited state of the SnTPP component. The absence of any related photoproducts clearly means that, similarly to the singlet radical pair, the ^{3}|SnTPP$^{\bullet-}$–TyrO$^{\bullet}$|···$^{+}$HPyr diradical disappears with faster kinetics.

Overall, the results obtained on conjugate **1** in CH_2Cl_2 with pyrrolidine under proper experimental conditions confirm that (i) as previously inferred[22] the quenching mechanism of both singlet and triplet excited states in **1** in CH_2Cl_2 in the presence of pyrrolidine does occur via a CPET mechanism; (ii) the kinetics of the forward CPET processes from both excited states are identical, within experimental error, to the one previously estimated; (iii) differently from what was previously proposed,[22] the recombination of both ^{1,3}|SnTPP$^{\bullet-}$–TyrO$^{\bullet}$|···$^{+}$HPyr diradical species is faster than its formation.

Effect of the Base on the Photoinduced PCET. We then tested the ability of Sn^{IV} di(L-tyrosinato) porphyrin conjugates to undergo photoinduced PCET quenching processes in CH_2Cl_2 by changing the thermodynamics of the formation of the radical pair state. Since the driving force for a PCET step (ΔG_{PCET}) is given by the sum of the driving forces for the electron transfer (ΔG_{ET}) and proton transfer (ΔG_{PT}) steps,[2] we first changed the energetic contribution of the protonation by investigating conjugate **1** in CH_2Cl_2 in combination with bases of progressively lower strength than pyrrolidine (Chart 2), namely, 4-dimethylaminopyridine

Chart 2. Molecular Structures of the Bases Used in the Present Study with Related pK_a

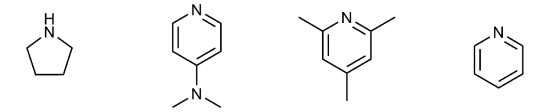

(DMAP, pK_a = 17.95 in acetonitrile)[23] and 2,4,6-trimethylpyridine (TMePy, pK_a = 14.98 in acetonitrile).[23] It should be pointed out that the use of bases of still lower strength, e.g., pyridine (pK_a = 12.53 in acetonitrile),[23] turns out to be ineffective in promoting photoinduced PCET processes in conjugate **1**.

Addition of increasing amounts of DMAP to a solution of **1** in CH_2Cl_2 causes a decrease of the fluorescence intensity of the SnTPP component (Figure 3A) and, correspondingly, of the singlet excited-state lifetime as measured by TC-SPC. The quenching efficiency saturates at a concentration of DMAP ≥ 25 mM, reaching a maximum yield of ca. 45% and a lifetime of τ = 0.59 ns for the singlet excited state. These results are characteristic of array **1** as negligible effects on the porphyrin fluorescence and lifetime are observed using model compound **2** in the presence of DMAP.

The experimental trend is similar to the one observed for **1** in the presence of pyrrolidine and can be attributed to the occurrence of a CPET quenching of the singlet excited state of the SnTPP chromophore, yielding a ^{1}|SnTPP$^{\bullet-}$–TyrO$^{\bullet}$|···$^{+}$HDMAP radical pair state. As a matter of fact,

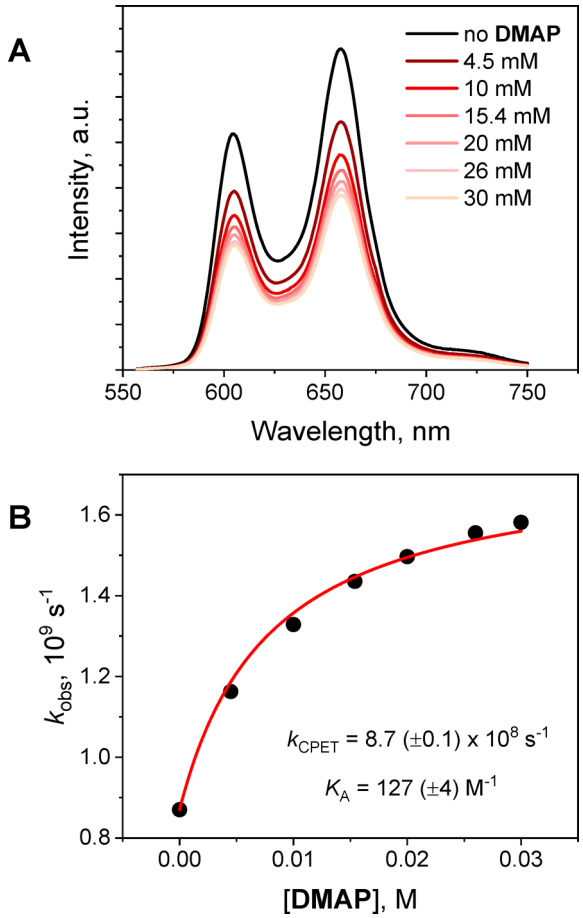

Figure 3. (A) Fluorescence spectra of 30 μM **1** in CH_2Cl_2 in the presence of 0–0.03 M DMAP (excitation at 535 nm) and (B) kinetic treatment of the singlet excited-state decay according to eq 1, using the reciprocal of the singlet excited-state lifetimes of **1** determined by TC-SPC (excitation at 600 nm, analysis at 660 nm).

treatment of the singlet decay rate according to eq 1, neglecting the bimolecular quenching term, proves effective in modeling the experimental data, yielding a rate constant of $k_{CPET,S1}$ = 8.7(±0.1) × 10^8 s^{-1} with an association constant of K_A = 127(±4) M^{-1} (Figure 3B).[42] This equilibrium constant is larger than the one obtained for the hydrogen bonding interaction between tyrosine and pyrrolidine and falls within the typical range of association constants between phenols and pyridines.[43,44] The presence of steric effects in pyrrolidine as well as the different p character of the lone pair in amine vs imine bases possibly explain the stronger hydrogen-bonding association experimentally observed for the tyrosine residue with DMAP when compared to pyrrolidine.[45−47] A KIE of 2.8(±0.2) has been determined for this quenching process when studied in CH_2Cl_2 in the presence of 1% CH_3OH or CD_3OD (Figure S28).

UFS measurements have been then performed on compound **1** in CH_2Cl_2 in the presence of DMAP. The results are reported in Figure S29 and are qualitatively similar to those observed in the presence of pyrrolidine (Figure 2), featuring a fast decay of the singlet excited state of the SnTPP component and formation of the related triplet state without apparent formation of CPET photoproducts. Similarly, this suggests that the diradical recombination of the ^{1}|SnTPP$^{\bullet-}$–TyrO$^{\bullet}$|···$^{+}$HDMAP is faster than formation. On a more

https://dx.doi.org/10.1021/acs.jpcc.0c00224
J. Phys. Chem. C 2020, 124, 8514−8525

quantitative basis, the amount of triplet formed is larger than that observed in the presence of pyrrolidine and the kinetics of the singlet excited-state decay slower (time constant of τ = 460 ps, Figure S29). Both observations are consistent with the less efficient quenching of the singlet excited state using DMAP (maximum yield of ca. 45%) as the base than that observed employing pyrrolidine (maximum yield of ca. 60%).[22]

The fate of the fraction of the triplet state formed in competition with the CPET singlet quenching has been then monitored by laser flash photolysis. The spectral evolution of **1** in CH_2Cl_2 in the presence of 33 mM DMAP (Figure S30) is comparable to the one observed with excess pyrrolidine (Figure S21A) and is characterized by a monotonic decay of the transient signal associated with the triplet excited state to the baseline. The triplet decay rate appreciably depends on the concentration of added DMAP, as monitored at the corresponding absorption maximum at 480 nm, reaching a maximum value at a concentration of ≥20 mM (Figure 4A).

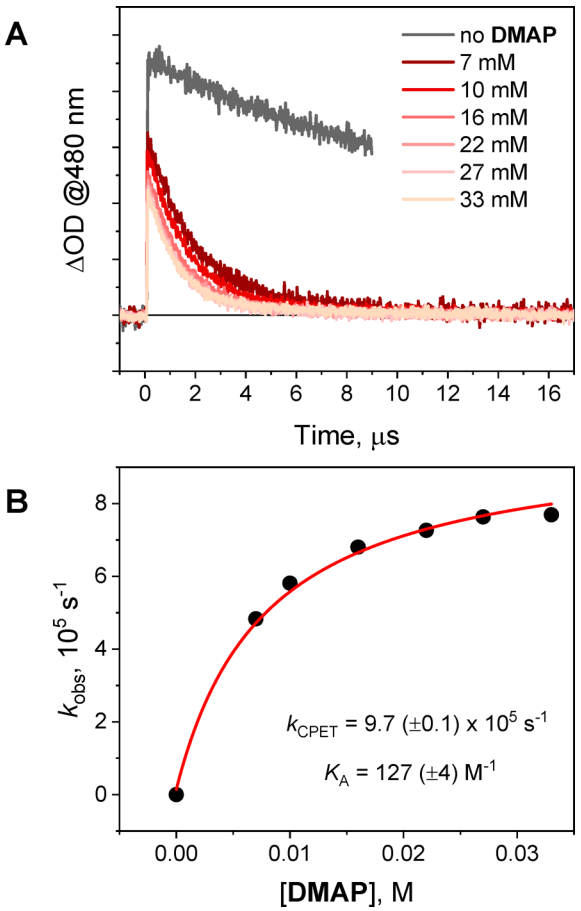

Figure 4. (A) Kinetic traces at 480 nm obtained by laser flash photolysis (excitation at 532 nm, 2 mJ) of 30 μM **1** in N_2-purged CH_2Cl_2 in the presence of 0−0.033 M DMAP and (B) kinetic treatment of the triplet excited-state decay according to eq 1 using the rates extracted from the fitting of the decays in Figure 4A.

Since no effect of DMAP is observed on the triplet excited-state lifetime of the SnTPP component in model compound **2**, these observations point toward the occurrence of a triplet CPET quenching pathway originating in **1** in the presence of the base. Consistently, a KIE of 2.0(±0.1) has been estimated when the triplet decays in the presence of DMAP are compared in 1% CH_3OH or CD_3OD (Figure S28). Furthermore, the triplet decay rates in **1** as a function of DMAP concentration can be well correlated using the kinetic formalism of eq 1 (neglecting the bimolecular contribution) using the same association constant of K_A = 127(±4) M^{-1} as for the singlet quenching, resulting in a rate constant of $k_{CPET,T1}$ = 9.7(±0.1) × 10^5 s^{-1} (Figure 4B). Akin to the pyrrolidine case, the failure to observe any signature of the ^{3}|SnTPP$^{\bullet-}$−TyrO$^{\bullet}$|···$^+$HDMAP diradical species in the laser flash photolysis experiment clearly confirms that the forward CPET quenching is the rate-determining step in the deactivation of the triplet excited state of the SnTPP component.

Addition of increasing amounts of the weaker base TMePy to a CH_2Cl_2 solution of **1** induces a progressive, albeit weak, quenching of the SnTPP fluorescence with a concomitant decrease of the singlet excited-state lifetime (Figure S31). The singlet quenching saturates at a base concentration of [TMePy] ≥ 15 mM, reaching a maximum efficiency of ca. 15%, considerably lower than that detected with **1** in the presence of both pyrrolidine and DMAP. A lifetime of 0.98 ns is attained for the singlet SnTPP at the largest concentration of TMePy employed. Akin to the pyrrolidine and DMAP cases, this experimental evidence is consistent with the occurrence of a CPET quenching of the singlet excited state of the SnTPP component with formation of a ^{1}|SnTPP$^{\bullet-}$−TyrO$^{\bullet}$|···$^+$TMePy diradical of singlet spin multiplicity. In agreement with the assignment made, negligible quenching of the singlet^1*SnTPP is observed with model compound **2** in the presence of TMePy. A KIE of 2.0(±0.2) has been measured when the singlet excited-state decay in the presence of TMePy is evaluated with 1% CH_3OH or CD_3OD (Figure S32). Also, treatment of the singlet decay rates using the formalism of eq 1 provides a nice correlation (Figure S31), yielding a rate constant of $k_{CPET,S1}$ = 2.0(±0.1) × 10^8 s^{-1} with an association constant of K_A = 125(±3) M^{-1}.[42] This equilibrium constant is within the same order of the values estimated in chlorinated solvents for the H-bond between TMePy and substituted phenols.[43,48,49]

The triplet excited state formed in almost quantitative yield, due to the intrinsically weak singlet CPET quenching, also decays with rates that depend on the concentration of added TMePy, showing a comparable saturation profile as observed for the singlet quenching channel (Figure S33). Similarly, this is consistent with the occurrence of a CPET quenching process from the triplet excited state of the SnTPP component in the presence of the TMePy base. A KIE of 1.6(±0.2) has been measured when the quenching process in the presence of TMePy is evaluated with 1% CH_3OH or CD_3OD (Figure S32). Furthermore, the kinetic formalism of eq 1 turns out to be effective in modeling the triplet excited-state decay rates in the presence of TMePy, providing a rate constant of $k_{CPET,T1}$ = 3.6(±0.1) × 10^4 s^{-1} with the same association constant of K_A = 125(±3) M^{-1} (Figure S33).[48,49] As for the product of this triplet CPET quenching, similarly to the pyrrolidine and DMAP cases, the spectral evolution monitored by laser flash photolysis of **1** in the presence of 0.018 M TMePy (Figure S33) points toward a rate-determining CPET step to achieve a triplet ^{3}|SnTPP$^{\bullet-}$−TyrO$^{\bullet}$|···$^+$TMePy species, with much faster diradical recombination.

The photophysical results obtained with **1** in CH_2Cl_2 in the presence of bases of different strength are summarized in Scheme 1.

https://dx.doi.org/10.1021/acs.jpcc.0c00224
J. Phys. Chem. C 2020, 124, 8514−8525

Scheme 1. Energy Level Diagram Showing the Photophysical Behavior of Conjugate 1 in CH_2Cl_2 Solution in the Presence of Bases of Different Strength (Green, Pyrrolidine; Red, DMAP; Blue, TMePy)[a]

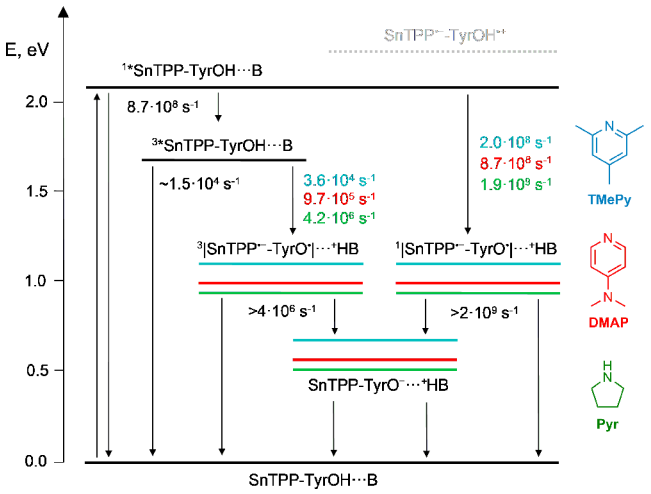

[a]The energy of the excited states has been taken from the literature,[24] and the energy of the PCET and PT-only states has been estimated considering the redox potentials experimentally determined (Table 1) and acid−base data for the base[23] and a phenol derivative[4,22] in acetonitrile.[50,51]

Conjugate 3 in CH_2Cl_2 with Pyrrolidine. We then moved to the investigation of conjugate **3** which displays a Sn^{IV} octaethylporphyrin chromophore *in lieu* of the tetraphenyl analogue. Introduction of ethyl groups increases the electron donation to the porphyrin core, thus making the macrocycle more difficult to reduce than the tetraphenylporphyrin.[24] This is indeed demonstrated by the reduction potential measured in **3** and **4** by CV, which appears at more negative values by ca. 0.2−0.3 V than their parent compounds **1** and **2**. Compared to the latter and using the same base, this change is expected to affect the driving force for the PCET processes (ΔG_{PCET}) in the Sn^{IV} di(L-tyrosinato) porphyrin conjugate via the energetic contribution from the redox step (ΔG_{ET}).

Addition of pyrrolidine to a CH_2Cl_2 solution containing conjugate **3** has negligible impact on both fluorescence intensity and singlet excited-state lifetime of the porphyrin component, thus suggesting that photoinduced CPET at the singlet level is not operative in the present system. On the other hand, increasing addition of pyrrolidine causes a faster decay of the triplet excited state of the SnOEP chromophore. As a matter of fact, as shown by laser flash photolysis measurements on conjugate **3** in CH_2Cl_2 in the presence of 0.07 M pyrrolidine (Figure 5A), the transient spectrum associated with the triplet excited state of the SnOEP component featuring absorption with maximum at 430 nm[24] decays to the baseline within ca. 10 μs. Since the effect of pyrrolidine on the excited state of the porphyrin component in model compound **4** is considerably less pronounced than that observed in conjugate **3** (a bimolecular quenching of k_Q = 3.4(±0.2) × 10^5 M^{-1} s^{-1} can be estimated from a Stern−Volmer analysis with model compound **4** and pyrrolidine, Figure S34), the observed behavior can be attributed to the occurrence of a CPET pathway implying the formation of a ^{3}|SnOEP$^{\bullet-}$−TyrO$^{\bullet}$|···$^+$HPyr diradical of triplet spin multiplicity.

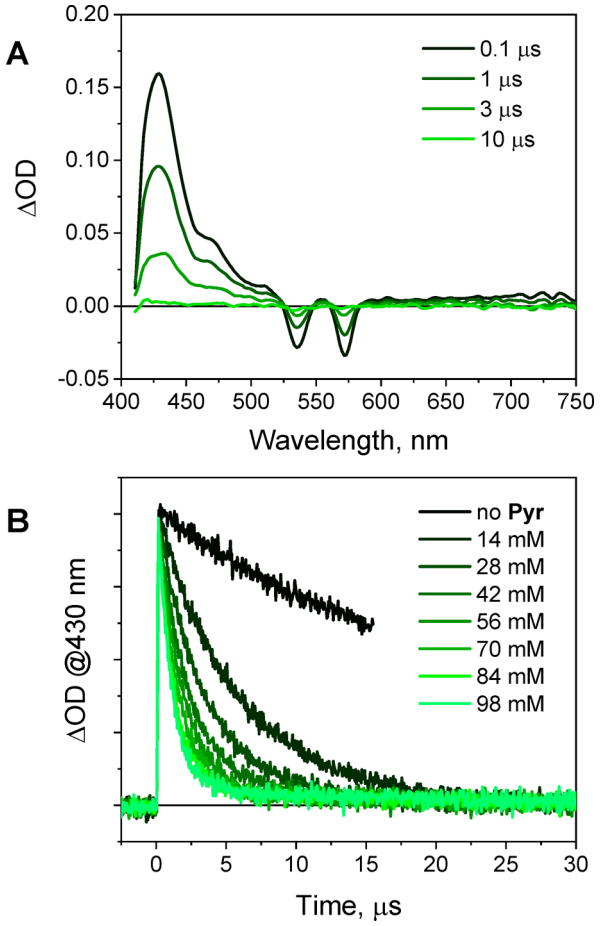

Figure 5. (A) Spectral evolution of the transient absorption obtained by laser flash photolysis (excitation at 532 nm, 2 mJ) of 10 μM **3** in N_2-purged CH_2Cl_2 in the presence of 0.07 M pyrrolidine and (B) kinetic traces at 430 nm with 0−0.098 M pyrrolidine.

Consistent with this hypothesis, the triplet decays (Figure 5B) display the characteristic saturation profile with respect to the base added, and the corresponding kinetic data can be modeled using the formalism in eq 1, employing a k_Q = 3.4(±0.2) × 10^5 M^{-1} s^{-1} and the association constant of K_A = 33.5 (±1.8) M^{-1} previously determined. This correlation (Figure S35) provides a rate constant of k_{CPET} = 8.4(±0.3) × 10^5 s^{-1} for the triplet CPET quenching process. A KIE of 1.3(±0.2) has been estimated for such a triplet quenching process when investigated in the presence of 1% CH_3OH or CD_3OD (Figure S36). Similar to conjugate **1**, no signature from the ^{3}|SnOEP$^{\bullet-}$−TyrO$^{\bullet}$|···$^+$Pyr diradical species is apparent, following the decay of the triplet excited state of the SnOEP component (Figure 5A). This suggests that formation of the radical pair state is slower than diradical recombination so that no accumulation of the CPET photoproducts can be attained.

The photophysical processes occurring in **3** in CH_2Cl_2 in the presence of pyrrolidine as a base are summarized in Scheme 2.

DISCUSSION

Conjugates **1** and **3** featuring a Sn^{IV} porphyrin chromophore bound to two L-tyrosine amino acids both display the ability to undergo photoinduced CPET processes when studied in CH_2Cl_2 in combination with a suitable organic base. Conjugate **1** can be quenched at both the singlet and triplet excited-state

https://dx.doi.org/10.1021/acs.jpcc.0c00224
J. Phys. Chem. C 2020, 124, 8514−8525

Scheme 2. Energy Level Diagram Showing the Photophysical Behavior of Conjugate 3 in CH_2Cl_2 Solution in the Presence of Pyrrolidine[a]

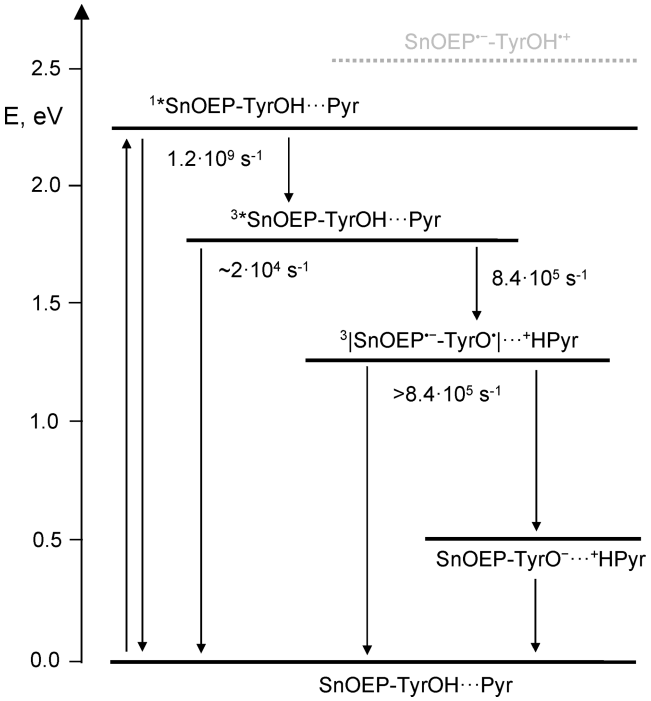

[a]The energy of the excited states has been taken from the literature,[24] and the energy of the PCET and PT-only states has been estimated considering the redox potentials experimentally determined (Table 1) and acid–base data for pyrrolidine[23] and a phenol derivative[4,22] in acetonitrile.[50,51]

level, and the rate and extent of both singlet and triplet quenching pathways depend on the strength of the base used. On the other hand, conjugate **3** can be quenched only at the triplet level in the presence of a strong base such as pyrrolidine. The failure to detect any appreciable singlet quenching in the latter very likely reflects both the poor efficiency of the singlet CPET quenching and the faster unimolecular excited-state decay of the SnOEP singlet than the SnTPP one. The involvement of both electron and proton motions in the quenching mechanism has been confirmed by means of kinetic modeling[30] as well as via the determination of KIEs working in the presence of 1% methanol or deuterated methanol.[35] As for the latter point, the KIEs obtained are in line with those previously found for CPET processes in related systems involving polypyridine complexes of rhenium(I) or ruthenium(II) covalently bound to phenol derivatives.[30,52] Although trends in KIEs are usually complex to rationalize due to the multiple variables that come into play,[2,3] in the present case larger KIEs have been observed in the case of **1** in combination with bases such as DMAP and TMePy for which higher association constants have been estimated. On the other hand, smaller KIE values have been observed with both **1** and **3** in the presence of pyrrolidine. The magnitude of the KIE is determined, to some extent, by the proton donor–acceptor distance and vibrational frequency.[53] Thus, it can be hypothesized that the different average N···H–O distances, expected to be smaller in the case of stronger hydrogen bonding donors, may represent a possible, relevant factor in determining the KIE.

The kinetic data obtained from the photophysical investigation can be correlated on a qualitative basis, quantitative comparisons being indeed hampered by the absence of reliable thermodynamic data for the acid–base equilibria in the chlorinated solvent for the proton donor/acceptor partners involved. A decrease of the driving force for the CPET quenching process (ΔG_{CPET}), as obtained by decreasing the base strength in **1** in CH_2Cl_2 from pyrrolidine to TMePy or by changing the porphyrin component from a tetraphenyl- to an octaethyl-substituted macrocycle when moving from **1** to **3** using pyrrolidine as a base, in all cases translates into a deceleration of the kinetics of both singlet (if any) and triplet excited-state quenching. Assuming a Marcus-type treatment for the CPET process,[2,19,54] these results can be explained considering that the forward photoinduced CPET step takes place in the normal (activated) region. The larger variation in rates observed in conjugate **1** upon decreasing the strength of the base when the triplet CPET processes ($k_{CPET,T1}$ between 4.2×10^6 and 3.6×10^4 s^{-1}) are compared to the singlet ones ($k_{CPET,S1}$ between 1.9×10^9 and 2.0×10^8 s^{-1}) very likely reflects the smaller driving forces in the former than in the latter that place the corresponding processes in the steepest portion of the Marcus parabola. Overall, this evidence is consistent with a reorganization energy of $\lambda \sim 1.2$ eV previously estimated for conjugate **1** in the presence of pyrrolidine,[22] considering available acid–base data for the base in acetonitrile as the solvent and using 2,4,6-tri-*tert*-butylphenol as a tyrosine model.[4,23] Large reorganization energies are indeed typical of CPET processes which imply substantial contribution from the proton transfer step.[2] Interestingly, the present results are also consistent with the large reorganization energy of $\lambda = 1.4$ eV measured in covalent anthracene–phenol dyad systems for which CPET in the inverted region has been observed for the first time.[21]

The more accurate investigation of the photophysical properties of conjugate **1** in the presence of pyrrolidine under proper experimental conditions as well as extension of the PCET studies to different bases (DMAP, TMePy, pyridine) and chromophore units (**3**) pointed toward the absence of any long-lived transient species of diradical nature. As a matter of fact, in all the systems examined, the photoinduced CPET quenching, both at the singlet (when present) and triplet level, represents the rate-determining step in the deactivation of the corresponding excited states. As to the ground-state decay of the intermediate diradical species formed, although this work does not provide direct evidence thereof, the radical pair states are expected to decay to the ground state via a stepwise PT-ET mechanism. This is indeed the typical behavior observed in previously investigated systems involving covalent chromophore–phenol dyads.[30] In this respect, both conjugates **1** and **3**, in combination with suitable organic bases, actually behave as photoacids. As a matter of fact, considering the energy of both PCET and PT-only states (with the benefit of error arising from the absence of reliable acid–base data in CH_2Cl_2) as well as the typical reorganization energies of Sn^{IV} porphyrin-based systems involving simple ET processes ($\lambda \sim 0.5$ eV),[55] diradical recombination in both **1** and **3** to a SnP–TyrO$^-$···$^+$HB "proton transfer" state is expected to be close to the activationless regime and thus substantially fast.

https://dx.doi.org/10.1021/acs.jpcc.0c00224
J. Phys. Chem. C 2020, 124, 8514–8525

CONCLUSION

Conjugates **1** and **3**, featuring a Sn^{IV} porphyrin chromophore axially connected to two L-tyrosinato amino acidic residues, have been characterized in the context of photoinduced PCET. Detailed analysis of the photoinduced dynamics has been provided by a series of time-resolved spectroscopic techniques in both the ultrafast and fast time regime. Reinvestigation of the photophysics of **1** in CH_2Cl_2 in the presence of pyrrolidine shows that both singlet and triplet excited states are quenched by CPET, but no radical pair state can be produced for kinetic reasons (diradical recombination faster than formation). Lowering the strength of the base used with **1**, going from pyrrolidine to DMAP to TMePy, causes a substantial decrease of both singlet and triplet CPET quenching rates and efficiencies. The photophysical behavior of **3** in CH_2Cl_2 with pyrrolidine has been also studied showing negligible quenching of the singlet excited state and efficient quenching at the triplet level, albeit with slower rates than observed with its parent conjugate **1**, resulting from the smaller driving force for the forward CPET step. Overall, the trend in CPET kinetics can be well correlated, adopting Marcus-type considerations, and is consistent with the involvement of substantial reorganization energy in the forward CPET reactions. Although long-lived diradical species cannot be achieved, as previously hypothesized, the present work still highlights the potential of simple, supramolecular systems toward the comprehension and understanding of the mechanistic requirements at the basis of PCET reactions.

ASSOCIATED CONTENT

Supporting Information

The Supporting Information is available free of charge at https://pubs.acs.org/doi/10.1021/acs.jpcc.0c00224.

Characterization (1D and 2D NMR, ESI-MS, CD) of **3**, photophysics and electrochemistry in CH_2Cl_2, KIE studies, and other photophysical studies (PDF)

AUTHOR INFORMATION

Corresponding Authors

Mirco Natali − *Department of Chemical and Pharmaceutical Sciences, University of Ferrara, and Centro Interuniversitario per la Conversione Chimica dell'Energia Solare (SolarChem), sez. di Ferrara, 44121 Ferrara, Italy*; orcid.org/0000-0002-6638-978X; Email: mirco.natali@unife.it

Elisabetta Iengo − *Department of Chemical and Pharmaceutical Sciences, University of Trieste, 34127 Trieste, Italy*; Email: eiengo@units.it

Authors

Agnese Amati − *Department of Chemical and Pharmaceutical Sciences, University of Trieste, 34127 Trieste, Italy*

Sebastiano Merchiori − *Department of Chemical and Pharmaceutical Sciences, University of Ferrara, and Centro Interuniversitario per la Conversione Chimica dell'Energia Solare (SolarChem), sez. di Ferrara, 44121 Ferrara, Italy*

Barbara Ventura − *ISOF-CNR, 40129 Bologna, Italy*; orcid.org/0000-0002-8207-1659

Complete contact information is available at: https://pubs.acs.org/10.1021/acs.jpcc.0c00224

Author Contributions

The manuscript was written through contributions of all authors.

Notes

The authors declare no competing financial interest.

ACKNOWLEDGMENTS

M.N. acknowledges the University of Ferrara for funding (FAR2019). B.V. acknowledges the Italian CNR for funding (Project "PHEEL"). E.I. acknowledges the University of Trieste for funding (FRA2016).

ABBREVIATIONS

ET, electron transfer; PT, proton transfer; PCET, proton-coupled electron transfer; CPET, concerted proton−electron transfer; KIE, kinetic isotope effect; UFS, ultrafast spectroscopy; DMAP, 4-dimethylaminopyridine; TMePy, 2,4,6-trimethylpyridine.

REFERENCES

(1) Dempsey, J. L.; Winkler, J. R.; Gray, H. B. Proton Coupled Electron Transfer Flow in Protein Machines. *Chem. Rev.* **2010**, *110*, 7024−7039.

(2) Huynh, M. H. V.; Meyer, T. J. Proton Coupled Electron Transfer. *Chem. Rev.* **2007**, *107*, 5004−5064.

(3) Weinberg, D. R.; Gagliardi, C. J.; Hull, J. F.; Murphy, C. F.; Kent, C. A.; Westlake, B. C.; Paul, A.; Ess, D. H.; McCafferty, D. G.; Meyer, T. J. Proton Coupled Electron Transfer. *Chem. Rev.* **2012**, *112*, 4016−4093.

(4) Warren, J. J.; Tronic, T. A.; Mayer, J. M. Thermochemistry of Proton Coupled Electron Transfer Reagents and its Implications. *Chem. Rev.* **2010**, *110*, 6961−7001.

(5) Costentin, C.; Robert, M.; Savéant, J.-M. Concerted Proton Electron Transfers: Electrochemical and Related Approaches. *Acc. Chem. Res.* **2010**, *43*, 1019−1029.

(6) Costentin, C.; Robert, M.; Savéant, J.-M. Electrochemical Concerted Proton and Electron Transfers. Potential-Dependent Rate Constant, Reorganization Factors, Proton Tunneling and Isotope Effects. *J. Electroanal. Chem.* **2006**, *588*, 197−206.

(7) Gagliardi, C. J.; Binstead, R. A.; Thorp, H. H.; Meyer, T. J. Concerted Electron-Proton Transfer (EPT) in the Oxidation of Tryptophan with Hydroxide as a Base. *J. Am. Chem. Soc.* **2011**, *133*, 19594−19597.

(8) Fecenko, C. J.; Thorp, H. H.; Meyer, T. J. The Role of Free Energy Change in Coupled Electron-Proton Transfer. *J. Am. Chem. Soc.* **2007**, *129*, 15098−15099.

(9) Gagliardi, C. J.; Murphy, C. F.; Binstead, R. A.; Thorp, H. H.; Meyer, T. J. Concerted Electron-Proton Transfer (EPT) in the Oxidation of Cysteine. *J. Phys. Chem. C* **2015**, *119*, 7028−7038.

(10) Zhang, M.-T.; Hammarström, L. Proton-Coupled Electron Transfer from Tryptophan: A Concerted Mechanism with Water as Proton Acceptor. *J. Am. Chem. Soc.* **2011**, *133*, 8806−8809.

(11) Dongare, P.; Maji, S.; Hammarström, L. Direct Evidence of a Tryptophan Analogue Radical Formed in a Concerted Electron-Proton Transfer Reaction in Water. *J. Am. Chem. Soc.* **2016**, *138*, 2194−2199.

(12) Irebo, T.; Reece, S. Y.; Sjödin, M.; Nocera, D. G.; Hammarström, L. Proton Coupled Electron Transfer of Tyrosine Oxidation: Buffer Dependence and Parallel Mechanisms. *J. Am. Chem. Soc.* **2007**, *129*, 15462−15464.

(13) Irebo, T.; Zhang, M.-T.; Markle, T. F.; Scott, A. M.; Hammarström, L. Spanning Four Mechanistic Regions of Intramolecular Proton Couple Electron Transfer in a $Ru(bpy)_3^{2+}$-Tyrosine Complex. *J. Am. Chem. Soc.* **2012**, *134*, 16247−16254.

(14) Reece, S.; Nocera, D. G. Direct Tyrosine Oxidation using the MLCT Excited States of Rhenium Polypyridyl Complexes. *J. Am. Chem. Soc.* **2005**, *127*, 9448−9458.
(15) Wenger, O. S. Proton Coupled Electron Transfer Originating from Excited States of Luminescent Metal Complexes. *Chem. - Eur. J.* **2011**, *17*, 11692−11702.
(16) Pannwitz, A.; Wenger, O. S. Photoinduced Electron Transfer Coupled to Donor Deprotonation and Acceptor Protonation in a Molecular Triad Mimicking Photosystem II. *J. Am. Chem. Soc.* **2017**, *139*, 13308−13311.
(17) Pannwitz, A.; Wenger, O. S. Recent Advances in Bioinspired Proton-Coupled Electron Transfer. *Dalton Trans* **2019**, *48*, 5861−5868.
(18) Lennox, J. C.; Kurtz, D. A.; Huang, T.; Dempsey, J. L. Excited State Proton Coupled Electron Transfer: Different Avenues for Promoting Proton/Electron Movements with Solar Photons. *ACS Energy Lett.* **2017**, *2*, 1246−1256.
(19) Schrauben, J. N.; Cattaneo, M.; Day, T. C.; Tenderholt, A. L.; Mayer, J. M. Multiple-Site Concerted Proton-Electron Transfer Reactions of Hydrogen-Bonded Phenols are Non-Adiabatic and Well Described by Semiclassical Marcus Theory. *J. Am. Chem. Soc.* **2012**, *134*, 16635−16645.
(20) Bowring, M. A.; Bradshaw, L. R.; Parada, G. A.; Pollock, T. P.; Fernández-Terán, R. J.; Kolmar, S. S.; Mercado, B. Q.; Schlenker, C. W.; Gamelin, D. R.; Mayer, J. M. Activationless Multiple-Site Concerted Proton-Electron Tunneling. *J. Am. Chem. Soc.* **2018**, *140*, 7449−7452.
(21) Parada, G. A.; Goldsmith, Z. K.; Kolmar, S.; Pettersson Rimgard, B.; Mercado, B. Q.; Hammarström, L.; Hammes-Schiffer, S.; Mayer, J. M. Concerted Proton-Electron Transfer Reactions in the Marcus Inverted Region. *Science* **2019**, *364*, 471−475.
(22) Natali, M.; Amati, A.; Demitri, N.; Iengo, E. Formation of a Long-Lived Radical Pair in a Sn(IV) Porphyrin-di(L-tyrosinato) Conjugate Driven by Proton-Coupled Electron-Transfer. *Chem. Commun.* **2018**, *54*, 6148−6152.
(23) Kaljurand, I.; Kütt, A.; Soovali, L.; Rodima, T.; Maemets, V.; Leito, I.; Koppel, I. A. Extension of the Self-Consistent Spectrophotometric Basicity Scale in Acetonitrile to a Full Span of 28 pKa Units: Unification of Different Basicity Scales. *J. Org. Chem.* **2005**, *70*, 1019−1028.
(24) Amati, A.; Cavigli, P.; Demitri, N.; Natali, M.; Indelli, M. T.; Iengo, E. Sn(IV) Multiporphyrin Arrays as Tunable Photoactive Systems. *Inorg. Chem.* **2019**, *58*, 4399−4411.
(25) Natali, M.; Argazzi, R.; Chiorboli, C.; Iengo, E.; Scandola, F. Photocatalytic Hydrogen Evolution with a Self-Assembling Reductant-Sensitizer-Catalyst System. *Chem. - Eur. J.* **2013**, *19*, 9261−9271.
(26) Natali, M.; Orlandi, M.; Chiorboli, C.; Iengo, E.; Bertolasi, V.; Scandola, F. Porphyrin-Cobaloxime Dyads for Photoinduced Hydrogen Production: Investigation of the Primary Photochemical Process. *Photochem. Photobio. Sci.* **2013**, *12*, 1749−1753.
(27) Amati, A.; Cavigli, P.; Kahnt, A.; Indelli, M. T.; Iengo, E. A Self-assembled Ruthenium(II)Porphyrin-Aluminium(III)Porphyrin-Fullerene Triad for Long-lived Photoinduced Charge Separation. *J. Phys. Chem. A* **2017**, *121*, 4242−4252.
(28) Indelli, M. T.; Chiorboli, C.; Ghirotti, M.; Orlandi, M.; Scandola, F.; Kim, H. J.; Kim, H.-J. Photoinduced Electron Transfer in Ruthenium(II)/Tin(IV) Multiporphyrin Arrays. *J. Phys. Chem. B* **2010**, *114*, 14273−14282.
(29) Iengo, E.; Pantoş, G. D.; Sanders, J. K. M.; Orlandi, M.; Chiorboli, C.; Fracasso, S.; Scandola, F. A Fully Self-Assembled Non-Symmetric Triad for Photoinduced Charge Separation. *Chem. Sci.* **2011**, *2*, 676−685.
(30) Chen, J.; Kuss-Petermann, M.; Wenger, O. S. Distance Dependence of Bidirectional Concerted Proton-Electron Transfer in Phenol-Ru(2,2'-bipyridine)$_3^{2+}$ Dyads. *Chem. - Eur. J.* **2014**, *20*, 4098−4104.
(31) This correction was not taken into consideration in our previous determination of the K_A via a spectrophotometric technique.[22] Indeed, although its contribution is intrinsically weak, it has a non-negligible role in the actual value of the association constant.
(32) Miyasaka, H.; Tabata, A.; Ojima, S.; Ikeda, N.; Mataga, N. Femtosecond-Picosecond Laser Photolysis Studies on the Mechanisms of Fluorescence Quenching Induced by Hydrogen-Bonding Interactions − 1-Pyrenol-Pyridine Systems. *J. Phys. Chem.* **1993**, *97*, 8222−8228.
(33) Dongare, P.; Bonn, A. G.; Maji, S.; Hammarström, L. Analysis of Hydrogen-Bonding Effects on Excited State Proton-Coupled Electron-Transfer from a Series of Phenols to a Re(I) Polypyridyl Complex. *J. Phys. Chem. C* **2017**, *121*, 12569−12576.
(34) Petersson, J.; Hammarström, L. Ultrafast Electron Transfer Dynamics in a Series of Porphyrin/Viologen Complexes: Involvement of Electronically Excited Radical Pair Products. *J. Phys. Chem. B* **2015**, *119*, 7531−7540.
(35) Markle, T. F.; Rhile, I. J.; Mayer, J. M. Kinetic Effects of Increased Proton Transfer Distance on Proton-Coupled Oxidation of Phenol Amines. *J. Am. Chem. Soc.* **2011**, *133*, 17341−17352.
(36) Harriman, A.; Richoux, R. C.; Neta, P. Redox Chemistry of Metalloporphyrins in Aqueous Solution. *J. Phys. Chem.* **1983**, *87*, 4957−4965.
(37) Kadish, K. M.; Xu, Q. Y. Y.; Maiya, G. B.; Barbe, J.-M.; Guilard, R. Effects of Axially Bound Anions on the Electroreduction of Tin(IV) Porphyrins in Tetrahydrofuran. *J. Chem. Soc., Dalton Trans.* **1989**, 1531−1536.
(38) Hviid, L.; Bouwman, W. G.; Paddon-Row, M. N.; Van Ramesdonk, H. J.; Verhoeven, J. W.; Brouwer, A. M. Spin Control of the Lifetime of an Intramolecular Charge Transfer State. *Photochem. Photobio. Sci.* **2003**, *2*, 995−1001.
(39) Verhoeven, J. W. On the Role of Spin Correlation in the Formation, Decay, and Detection of Long-Lived, Intramolecular Charge Transfer States. *J. Photochem. Photobiol., C* **2006**, *7*, 40−60.
(40) Amati, A.; Natali, M.; Indelli, M. T.; Iengo, E.; Würthner, F. Photoinduced Energy- and Electron-Transfer Processes in a Side-to-Face Ru^{II}-Porphyrin/Perylene Bisimide Array. *ChemPhysChem* **2019**, *20*, 2195−2203.
(41) The nature of the actual species formed upon laser excitation of conjugate **1**, in either the absence or presence of the base, has not been identified yet. We can only postulate that it may be related to an irreversible formation of some porphyrin-related photoproducts as confirmed from the comparison of the absorption spectra of **1** before and after a long-term exposure to 532 nm laser pulses (Figure S36). The presence of impurities in the pristine compound, possibly contributing in the photochemical reaction, can be ruled out according to the H-Sn HMBC experiments. As for the mechanism of the formation of this species, this is also presently unclear, but the strong dependence of its contribution in the transient absorption experiments (*vide infra*) on the laser power, along with the absence of any substantial quenching of both singlet and triplet excited states in **1**, when compared to its model compound **2**, likely suggests the occurrence of a photoinduced chain reaction originating from a nonlinear process, with the possible involvement of the acidic hydroxide groups of the tyrosine amino acids. Importantly, the role of the CH_2Cl_2 solvent in this detrimental photoinduced reaction does not appear as a major one since enhanced degradation is observed in acetonitrile solution.
(42) Independent determination of the association constant using UV−vis spectroscopy, as made with pyrrolidine, cannot be performed in the present case due to the overlaying absorption of the base with the tyrosine bands.
(43) Biczok, L.; Gupta, N.; Linschitz, H. Coupled Electro-Proton Transfer in Interactions of Triplet C_{60} with Hydrogen-Bonded Phenols: Effects of Solvation, Deuteration, and Redox Potentials. *J. Am. Chem. Soc.* **1997**, *119*, 12601−12609.
(44) Gurka, D.; Taft, R. W. Studies of Hydrogen-Bonding Formation with *p*-Fluorophenol. IV. The Fluorine Nuclear Magnetic Resonance Method. *J. Am. Chem. Soc.* **1969**, *91*, 4794−4801.
(45) It should be considered that, albeit related, the hydrogen-bonding basicity (i.e., the ability to act as a hydrogen-bonding

https://dx.doi.org/10.1021/acs.jpcc.0c00224
J. Phys. Chem. C 2020, 124, 8514−8525

acceptor) might be different from the Brønsted basicity. As a matter of fact, the steric hindrance, the p character of the lone pair, and the presence of intramolecular interactions[46] may contribute to the hydrogen-bonding basicity in addition to the intrinsic Brønsted basicity of the base. Consistent with the association constant experimentally determined, theoretical calculations[46,47] estimate that the hydrogen-bonding-accepting character of DMAP is indeed larger than the one of pyrrolidine.

(46) Graton, J.; Berthelot, M.; Laurence, C. Hydrogen-Bond Basicity pK_{HB} Scale of Secondary Amine. *J. Chem. Soc., Perkin. Trans.* **2001**, *2*, 2130−2135.

(47) Graton, J.; Le Questel, J.-Y.; Maxwell, P.; Popelier, P. Hydrogen-Bond Accepting Properties of New Heteroaromatic Ring Chemical Motifs: A Theoretical Study. *J. Chem. Inf. Model.* **2016**, *56*, 322−334.

(48) Since the hydrogen-bonding-accepting character of TMePy is expected to be smaller than the one of DMAP,[49] a smaller association constant would be envisioned. In the present case, the poorly efficient CPET quenching of both singlet and triplet excited states experimentally measured for TMePy together with the error associated with the lifetime determination makes the K_A estimated via this procedure not as accurate as the one estimated for DMAP. As an example, with an error of ±2% on the lifetimes measured for both the singlet and triplet excited states with TMePy and using the k_{CPET} estimated from eq 1 (see text), an association constant ranging between ∼50 and ∼150 M^{-1} may actually model the CPET kinetics to a satisfactory extent. Precise determination of the association constant K_A between tyrosine and TMePy is, however, out of the scope of this work.

(49) Green, A. J.; Popelier, P. L. A. Theoretical Prediction of Hydrogen-Bond Basicity pK_{BHX} Using Quantum Chemical Topology Descriptors. *J. Chem. Inf. Model.* **2014**, *54*, 553−561.

(50) The energy of the PCET state has been estimated considering the energy of the charge-transfer state without base (estimated from the redox data in Table 1) and subtracting the contribution from the deprotonation step: $\Delta G_{PT} = 0.059\ eV\cdot[pK_a(TyrOH^{\bullet+}) - pK_a(^{+}HB)]$. For the sake of simplicity, the same energy has been assumed for the singlet and triplet radical pair states. In the absence of suitable pK_a data in CH_2Cl_2, we decided to consider pK_a values for both acids in acetonitrile.[4,23] The 2,4,6-tri-*tert*-butylphenoxyl radical[4] was used in place of $TyrOH^{\bullet+}$, whose pK_a value is unknown. While absolute pK_a data might differ substantially when moving from one solvent to another one, ΔpK_a values correlate well among different organic solvents,[51] so that the ΔG_{PT} estimated can be confidently employed to construct a reliable energy level diagram. The energy of the PT-only state has been estimated according to the following equation: $\Delta G_{PT} = 0.059\ eV\cdot[pK_a(TyrOH) - pK_a(^{+}HPyr)]$, using the pK_a of 2,4,6-tri-*tert*-butylphenol[4] for TyrOH.

(51) Kutt, A.; Selberg, S.; Kaljurand, I.; Tshepelevitsh, S.; Heering, A.; Darnell, A.; Kaupmees, K.; Piirsalu, M.; Leito, I. pK_a Values in Organic Chemistry − Making Maximum Use of the Available Data. *Tetrahedron Lett.* **2018**, *59*, 3738−3748.

(52) Kuss-Petermann, M.; Wolf, H.; Stalke, D.; Wenger, O. S. Influence of Donor-Acceptor Distance Variation on Photoinduced Proton and Electron Transfer in Rhenium(I)-Phenol Dyads. *J. Am. Chem. Soc.* **2012**, *134*, 12844−12854.

(53) Edwards, S. J.; Soudackov, A. V.; Hammes-Schiffer, S. Analysis of Kinetic Isotope Effects for Proton-Coupled Electron Transfer Reactions. *J. Phys. Chem. A* **2009**, *113*, 2117−2126.

(54) Mayer, J. M. Simple Marcus-Theory-Type Model for Hydrogen-Atom Transfer/Proton-Coupled Electro Transfer. *J. Phys. Chem. Lett.* **2011**, *2*, 1481−1489.

(55) Kojima, T.; Hanabusa, K.; Ohkubo, K.; Shiro, M.; Fukuzumi, S. Construction of Sn^{IV} Porphyrin/trinuclear Ruthenium Cluster Dyads Linked via Pyridine Carboxylates: Photoinduced Electron Transfer in the Marcus Inverted Region. *Chem. - Eur. J.* **2010**, *16*, 3646−3655.

https://dx.doi.org/10.1021/acs.jpcc.0c00224
J. Phys. Chem. C 2020, 124, 8514−8525